

Molecular changes in neurons in multiple sclerosis: Altered axonal expression of Na_v1.2 and Na_v1.6 sodium channels and Na⁺/Ca²⁺ exchanger

Matthew J. Craner^{*†}, Jia Newcombe[‡], Joel A. Black^{*†}, Caroline Hartle[‡], M. Louise Cuzner[‡], and Stephen G. Waxman^{*†§}

^{*}Department of Neurology and Paralyzed Veterans of America/Eastern Paralyzed Veterans Association Neuroscience Research Center, Yale School of Medicine, New Haven, CT 06510; [†]Rehabilitation Research Center, Veterans Affairs Medical Center, West Haven, CT 06516; and [‡]Department of Neuroinflammation, Institute of Neurology, University College London, London WC1N 3BG, United Kingdom

Communicated by Dominick P. Purpura, Albert Einstein College of Medicine, Bronx, NY, April 19, 2004 (received for review February 12, 2004)

Although voltage-gated sodium channels are known to be deployed along experimentally demyelinated axons, the molecular identities of the sodium channels expressed along axons in human demyelinating diseases such as multiple sclerosis (MS) have not been determined. Here we demonstrate changes in the expression of sodium channels in demyelinated axons in MS, with Na_v1.6 confined to nodes of Ranvier in controls but with diffuse distribution of Na_v1.2 and Na_v1.6 along extensive regions of demyelinated axons within acute MS plaques. Using triple-labeled fluorescent immunocytochemistry, we also show that Na_v1.6, which is known to produce a persistent sodium current, and the Na⁺/Ca²⁺ exchanger, which can be driven by persistent sodium current to import damaging levels of calcium into axons, are colocalized with β -amyloid precursor protein, a marker of axonal injury, in acute MS lesions. Our results demonstrate the molecular identities of the sodium channels expressed along demyelinated and degenerating axons in MS and suggest that coexpression of Na_v1.6 and Na⁺/Ca²⁺ exchanger is associated with axonal degeneration in MS.

demyelinating diseases | action potential conduction | axonal degeneration

Nine genes encode distinct voltage-gated sodium channels (Na_v1.1–Na_v1.9) with a common motif but with different amino acid sequences and physiological characteristics (1). Na_v1.6 is the major sodium channel, which is clustered at the nodes of Ranvier (2), although Na_v1.2 is also present at some nodes (3, 4). However, the identity of sodium-channel isoforms that are present along demyelinated axons in disorders such as multiple sclerosis (MS) has not been established. In MS, the loss of myelin produces failure of axonal action-potential conduction that is associated with clinical exacerbations, but axonal conduction can recover as a result of expression of new sodium channels along demyelinated axons, providing a substrate for remission of clinical deficits (5). Axonal degeneration also occurs in MS, contributes to persistent neurological deficits (6–9), and may involve persistently activated sodium channels that drive injurious reverse Na⁺/Ca²⁺ exchange (10, 11). Blocking of sodium channels prevents axonal degeneration within white matter tracts in a variety of disease models (11–17), including a model of MS, experimental autoimmune encephalomyelitis (EAE) (18, 19).

During the development of myelinated CNS tracts, Na_v1.2 channels [which are also present along unmyelinated axons (3, 20, 21)] are initially expressed along premyelinated axons, with a transition to clusters of Na_v1.6 at mature nodes of Ranvier (3, 22). In dysmyelinated axons from *Shiverer* mice, Na_v1.2 channels are retained, and Na_v1.6 is not expressed (3, 23), and in axons from *Plp*^{-/-} mice, which myelinate normally and then lose their myelin, there is a loss of Na_v1.6 clustering and increased expression of Na_v1.2 (24). Electrophysiological (25), cytochemical (26), and immunocytochemical (27–29) studies using pan-specific sodium-channel antibodies demonstrate a higher-than-normal

density of sodium channels in chronically demyelinated axons but do not reveal the isoforms of the channels. A 4-fold increase in saxitoxin-binding sites in demyelinated white matter from MS patients also suggests the deployment of new Na channels (30) but gives no clues about the channel isoform(s) that are expressed.

Recent studies have demonstrated up-regulated expression of Na_v1.2 and Na_v1.6 along extensive regions of demyelinated axons in EAE (4, 31). Na_v1.2 channels produce rapidly activating and inactivating currents (32–34) and appear to support action-potential conduction, which occurs before myelination (35, 36), suggesting that newly produced Na_v1.2 channels can support conduction in demyelinated axons. Na_v1.6 channels, on the other hand, produce a persistent current in addition to rapidly activating and inactivating currents (33, 37, 38), and Na_v1.6 is coexpressed together with the Na⁺/Ca²⁺ exchanger (NCX) along degenerating axons in EAE (31).

In this study, we present an analysis of Na_v1.6 and Na_v1.2 sodium channels, and of the NCX, in white matter from the human CNS, obtained postmortem from patients with secondary progressive MS, and from control subjects with no neurological disease. We demonstrate that there are changes in the pattern of expression of sodium channels along demyelinated CNS axons in MS, with expression of Na_v1.6 confined to nodes of Ranvier in control white matter and with diffuse expression of both Na_v1.2 and Na_v1.6 along extensive regions of demyelinated axons in MS. We also show that Na_v1.6 (but not Na_v1.2), coexpressed with the NCX, is associated with axonal injury in MS.

Materials and Methods

MS Tissue. Postmortem cervical spinal cord and optic nerve tissue, acquired by means of a rapid protocol from patients with disabling secondary progressive MS ($n = 7$; 46.1 ± 6.5 yr, mean disease duration 14.0 ± 3.7 yr) and from controls ($n = 6$; 66.4 ± 6.0 yr) with no neurological disease, was obtained from the NeuroResource tissue bank (Institute of Neurology, London) (39); 1-cm³ tissue blocks were placed in OCT mounting medium (Lamb, London) on cork discs, then gently stirred for 9 s in isopentane precooled in liquid nitrogen before storage in airtight containers at -80°C . All tissue analyzed was characterized by oil red O and hematoxylin staining of 10 μm sections taken in triplicate, i.e., immediately before, in the middle, and immediately after serial sections cut from each tissue block. Acute MS lesions with ongoing or recent demyelination were identified on the basis of the presence of substantial numbers (graded as ≥ 3

Abbreviations: MS, multiple sclerosis; MBP, myelin basic protein; β -APP, β -amyloid precursor protein; NCX, Na⁺/Ca²⁺ exchanger; EAE, experimental autoimmune encephalomyelitis.
[§]To whom correspondence should be addressed at: Department of Neurology LCI 707, Yale School of Medicine, 15 York Street, New Haven, CT 06520-8018. E-mail: stephen.waxman@yale.edu.

© 2004 by The National Academy of Sciences of the USA

on a 0–5 scale) of oil red O-positive macrophages, containing neutral lipids resulting from myelin breakdown (40).

Immunocytochemistry. Tissue sections were processed for immunocytochemistry as described (4, 31). Briefly, sections were incubated simultaneously or in combination with anti-myelin basic protein (MBP) mouse IgG (1:4,000; Sternberger Monoclonals, Lutherville, MD), anti- β -amyloid precursor protein (β -APP) mouse IgG (1:100; Chemicon), anti-Caspr mouse IgG [1:500; provided by M. Rasband, University of Connecticut, Farmington (36)] or anti-NCX mouse IgM [NCX1 isoform, shown to be expressed in white matter axons (41)] (1:200; RDI, Flanders, NJ), anti-phosphorylated neurofilament (SMI-31, 1:20,000; Sternberger), anti-nonphosphorylated neurofilament (SMI-32, 1:20,000; Sternberger Monoclonals), and rabbit polyclonal antibodies to Na_v1.6 (residues 1042–1061; 1:100; Alomone, Jerusalem) or Na_v1.2 (residues 467–485; 1:100; Alomone). Sections were then washed in PBS, incubated with appropriate secondary antibodies, comprising goat anti-rabbit IgG-Cy3 (1:2,000; Amersham Biosciences), goat anti-mouse IgG-Alexa Fluor 488 (1:1,000; Molecular Probes), goat anti-mouse IgM-Alexa Fluor 488 (1:1,000; Molecular Probes), and goat anti-mouse IgG-Cy5 (1:200; Rockland, Gilbertsville, PA), in blocking solution for 3 h, washed in PBS, and mounted. Biotinylated *Ricinus communis* agglutinin 1 (1:200; Vector Laboratories) was used as a microglial/macrophage marker (42) and reacted with streptavidin-Cy5 (1:350; Amersham Biosciences) for detection. Control experiments, which included the omission of primary or secondary antibodies, showed no staining (data not shown).

Tissue Analysis. For analysis of sections, multiple representative images were accrued by confocal microscopy with a Nikon Eclipse E600 microscope. Analysis was confined to images in which axons were sectioned longitudinally as evident from the presence of linear (presumably demyelinated) axonal profiles with diffuse sodium-channel immunoreactivity, running for >20–30 μ m along the fiber tract within the plane of single sections.

In contrast to control white matter in which there was focal expression of Na_v1.6 and absence of Na_v1.2 at nodes of Ranvier (delineated by Caspr immunolabeling), we observed multiple extensive regions of diffuse Na_v1.2 and/or Na_v1.6 sodium-channel immunoreactivity along demyelinated (demonstrated by the lack of MBP immunostaining) axons (Figs. 1 and 2); neurofilament staining confirmed the axonal identity of these profiles (Fig. 2). As an index of the frequency of axonal profiles, we counted the number of these profiles that displayed diffuse regions of immunostaining for either Na_v1.2 or Na_v1.6, extending >10 μ m in length (therefore excluding nodal foci of immunostaining) as described (31). For quantification, a target line extending across the width of the image and perpendicular to the axis of the nerve fibers was overlaid on 10–18 randomly selected images (each 300 \times 300 μ m) per subject, and axonal profiles (>10- μ m length) with sodium-channel immunostaining that intersected the target line were counted. This approach was used in preference to expressing data per unit area because it negates the chance of duplicating quantification for a given axon as it moves in and out the tissue plane. An estimate of the number of injured axons per mm³ can be extrapolated from the data assuming a section thickness of 10 μ m and a window of 9 \times 10⁴ μ m² (300 μ m \times 300 μ m) for each image oriented perpendicular to the axis of the fiber tract. To facilitate the identification of immunopositive profiles and remove observer bias, quantitative microdensitometry was performed by using IPLAB image processing software (Scanalytics, Fairfax, VA) (4). Signal intensities were obtained by manually outlining profiles (10- to 15- μ m length) and, using IPLAB, we integrated densitometry function to

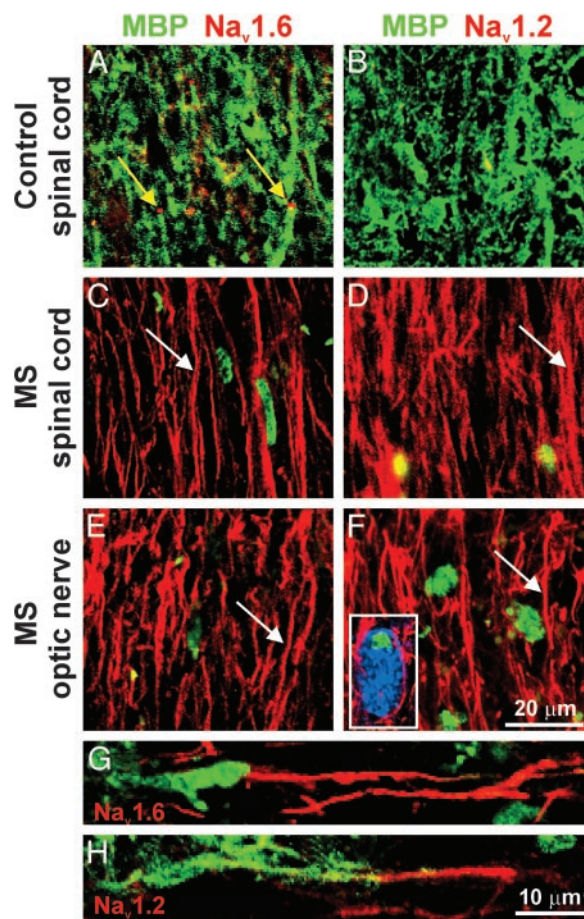


Fig. 1. Na_v1.6 and Na_v1.2 sodium channels are expressed along extensive regions of demyelinated axons in MS. Shown are representative images demonstrating sections of white matter from spinal cord (A–D) and optic nerve (E and F) immunostained for MBP (green) as a marker of myelination and for sodium channels Na_v1.6 (A, C, and E; red) and Na_v1.2 (B, D, and F; red). Control spinal cord white matter (A and B) demonstrates robust MBP immunostaining consistent with myelinated axons and does not display axonal profiles with diffuse (>10 μ m) sodium-channel immunostaining. Small foci of Na_v1.6 immunostaining (A; yellow arrows) are present, consistent with the focal distribution of Na_v1.6 at nodes of Ranvier in control spinal cord white matter, whereas Na_v1.2 immunostaining is absent (B). Within acute MS lesions from spinal cord (C and D) and optic nerve (E and F), there is significant demyelination as evident by marked attenuation of MBP immunostaining (residual foci of MBP immunostaining represent intracellular MBP products within macrophages, identified with *Ricinus communis* agglutinin 1 labeling; blue, F Inset). Multiple axonal profiles within these lesions display diffuse sodium-channel immunostaining (extending in many axons for >20 μ m; C, D, E, and F, white arrows) for Na_v1.6 (C and E) and Na_v1.2 (D and F). (G and H) Shown is the edge of active spinal cord plaques in MS and diffuse sodium-channel immunostaining for Na_v1.6 (G; red) and Na_v1.2 (H; red) along regions of axons where MBP immunostaining (green) is absent or markedly attenuated.

calculate mean signal intensities for the outlined areas. A profile was identified as a detectable linear outline extending for >10 μ m within the plane of section and as immunopositive if it displayed an optical intensity at least twice that of background levels. A minimum of 400 profiles per subject (control, $n = 3$; MS, $n = 4$) were identified (total 1,628 profiles examined in MS lesions) from multiple images. Statistical analysis was performed using the Student *t* test and the χ^2 test. The quantitative data presented represent the mean number of axonal profiles with diffuse Na_v1.2 or Na_v1.6 immunostaining \pm SEM per 600 μ m of target in control and MS spinal cord.

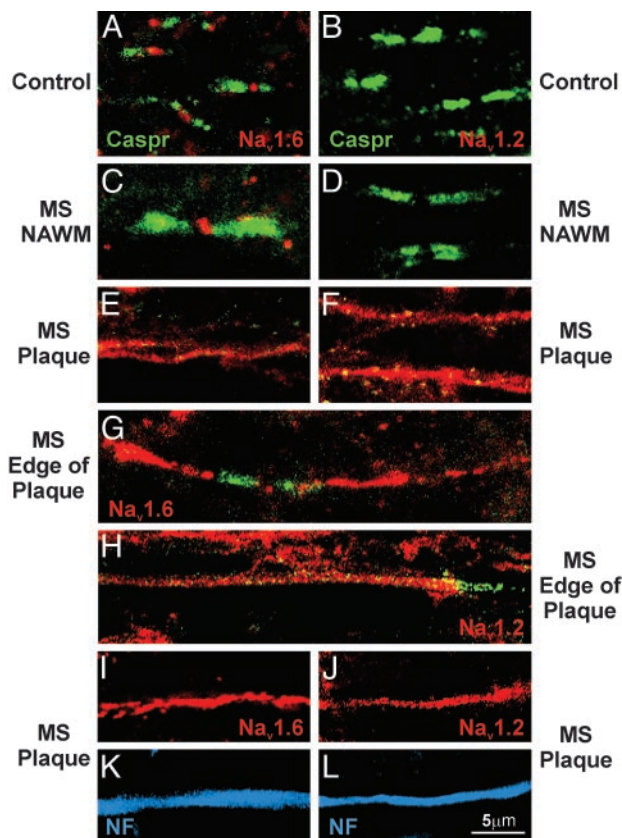


Fig. 2. $\text{Na}_v1.6$ and $\text{Na}_v1.2$ immunostaining in human control CNS and in MS. Shown are representative digital images of sections of postmortem spinal cord white matter from control (A and B) and MS (C–L) patients, immunostained to show $\text{Na}_v1.6$ (red), $\text{Na}_v1.2$ (red), Caspr (green), and neurofilaments (blue). In control white matter (A) and in normal-appearing white matter (NAWM) in MS tissue (C), $\text{Na}_v1.6$ is localized at nodes of Ranvier and is bounded by Caspr without appreciable overlap, whereas $\text{Na}_v1.2$ is not detectable (B and D). Within MS plaques, linear axonal profiles with continuous $\text{Na}_v1.6$ (E) and $\text{Na}_v1.2$ (F) immunostaining are present. In some instances an extensive zone of $\text{Na}_v1.6$ (G) or $\text{Na}_v1.2$ (H) immunostaining is bounded by Caspr, without overlap. Colocalization of $\text{Na}_v1.6$ (I) and $\text{Na}_v1.2$ (J) with neurofilament immunostaining (SMI 31/32; K and L; blue) further establishes the identity of these profiles as axons.

Results

$\text{Na}_v1.6$ and $\text{Na}_v1.2$ Sodium Channels Are Expressed Along Demyelinated Axons in Acute MS Plaques. Control white matter from patients with no neurological disease displayed abundant staining for MBP (Fig. 1 A and B) and a pattern of expression of $\text{Na}_v1.6$ and $\text{Na}_v1.2$ similar to the pattern in rodents. An antibody recognizing Caspr, an integral constituent of paranodal junctions that is believed to participate in demarcation of ion channel domains at nodes of Ranvier (43, 44), was used to delineate nodal regions. Examination of control spinal cord and optic nerve demonstrated focal $\text{Na}_v1.6$ immunostaining at nodes of Ranvier. The expression of $\text{Na}_v1.6$ was confined to nodal regions, and the nodal foci of $\text{Na}_v1.6$ immunostaining were bounded by Caspr without evidence of overlap, consistent with previous reports in rodents (2, 45) (Fig. 2A). Very few (<1%) nodes of Ranvier demonstrated $\text{Na}_v1.2$ immunostaining.

White matter from control spinal cords showed diffuse non-nodal (>10- μm length) $\text{Na}_v1.2$ immunolabeling of a small number of axons consistent with immunolabeling along unmyelinated fibers, which are known to express $\text{Na}_v1.2$ (3, 20, 21), with a total of 10.4 ± 1.2 axon profiles with diffuse $\text{Na}_v1.2$ immunostaining

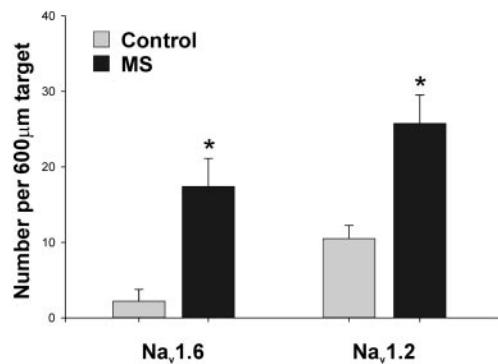


Fig. 3. Increased number of axons with extensive $\text{Na}_v1.6$ and $\text{Na}_v1.2$ immunostaining in MS spinal cord white matter. This histogram demonstrates a significant increase in the number of axons displaying diffuse sodium-channel immunostaining extending >10 μm along the fiber axis in MS spinal cord lesions. *, $P < 0.05$ compared with controls.

per 600- μm target. Only a very small number of axon profiles displayed diffuse $\text{Na}_v1.6$ immunostaining (2.2 ± 1.6 axon profiles per 600- μm target; Fig. 3); these did not express NCX or β -APP (data not shown) and are likely to represent nonmyelinated fibers, where $\text{Na}_v1.6$ is known to be expressed (46). Very low levels of NCX were detected at a small number of control nodes.

Acute MS lesions, identified by the presence of substantial numbers of oil red O-positive macrophages (40), displayed a distinctly different pattern of sodium-channel expression. Within MS lesions, there was a significant increase in the number of presumably demyelinated axons running along the fiber tract in regions of attenuated MBP immunostaining (Fig. 1 C–F), which display extensive (>10 μm) sodium-channel immunostaining. Fig. 2 I–L illustrates staining of these profiles for neurofilaments, establishing their identity as axons. Neurofilament staining occasionally demonstrated axonal tortuosity or swelling suggestive of injury, but this was not used to identify or quantitate injured axons, which were definitively identified by staining for β -APP (see below). In some cases, the extensive zone of $\text{Na}_v1.6$ or $\text{Na}_v1.2$ staining was bounded by Caspr (Fig. 2 G and H), which further confirmed the identity of the profile as an axon. As at normal nodes, there was no overlap between $\text{Na}_v1.6$ and Caspr immunostaining (Fig. 2 G and H). There was an 8-fold increase in the number of axons with diffuse $\text{Na}_v1.6$ immunostaining (17.4 ± 3.7 per 600- μm target; $P < 0.05$ compared with controls) and a 2.5-fold increase in the number of axons with $\text{Na}_v1.2$ immunostaining (25.8 ± 3.8 per 600- μm target; $P < 0.05$ compared with controls) within MS lesions in the spinal cord (Fig. 3). Similar changes were observed in the optic nerve of MS subjects (data not shown) where, importantly, unmyelinated fibers are not normally present (35).

Nodes of Ranvier within normal-appearing white matter from MS subjects appeared to display an arrangement similar to controls, with nodal foci of $\text{Na}_v1.6$ immunostaining bounded by Caspr (Fig. 2 C and D); a quantitative analysis of nodal immunoreactivity in normal-appearing white matter was not carried out.

$\text{Na}_v1.6$ Is Associated with Axonal Injury in MS. Studies in EAE (31) indicate that expression of $\text{Na}_v1.6$, but not $\text{Na}_v1.2$, over extended regions is associated with axonal injury. To delineate the relationship of $\text{Na}_v1.6$ compared with $\text{Na}_v1.2$ sodium-channel expression and axonal injury in MS, their colocalization with β -APP, a marker of axonal injury (7, 47, 48), was examined in spinal cord sections. Consistent with previous studies (7, 47, 48), we demonstrated evidence of axonal injury in acute MS lesions, with a 5-fold increase in the number of β -APP-positive axons

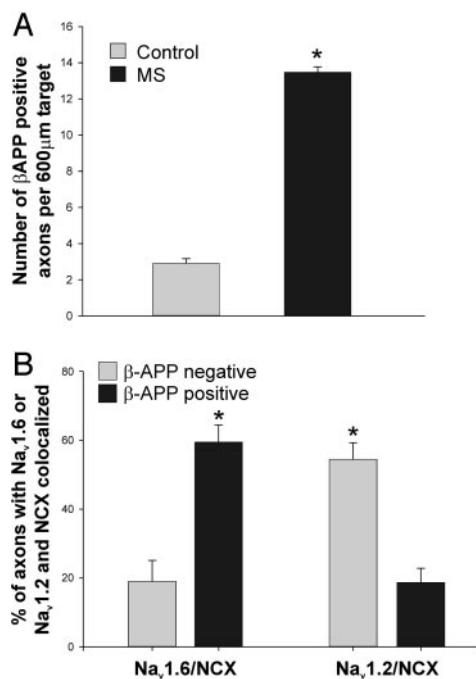


Fig. 4. (A) Increased β -APP expression in acute MS lesions. This histogram illustrates a significant increase in the number of axonal profiles that are β -APP-positive in MS. *, $P < 0.001$ compared with controls. (B) NCX and $\text{Na}_v1.6$ are coexpressed in β -APP-positive axons in MS. Triple immunolabeling was used to determine the proportion of β -APP-positive axons, and β -APP-negative axons, that coexpress NCX and $\text{Na}_v1.6$, or NCX and $\text{Na}_v1.2$, over extensive regions. The proportion of axons that coexpress $\text{Na}_v1.6$ and NCX is significantly higher in β -APP-positive axons than in β -APP-negative axons. *, $P < 0.005$.

(13.5 ± 0.3 per 600- μm target in MS, compared with 2.9 ± 0.3 per 600- μm target in controls; $P < 0.001$) (Fig. 4A). These β -APP-immunopositive axons in MS tended to express $\text{Na}_v1.6$ over extensive regions. Diffuse $\text{Na}_v1.6$ sodium-channel immunostaining was expressed in $82.3 \pm 3.2\%$ ($n = 4$ patients; 425 axons) of β -APP-immunopositive axons. In contrast, only $21.7 \pm 4.7\%$ ($n = 4$ patients; 309 axons, $P < 0.001$) of β -APP-immunopositive axons expressed diffuse $\text{Na}_v1.2$ sodium-channel immunostaining. Assuming a section thickness of 10 μm , our results suggest the presence of 7,500 injured axons per mm^3 of tissue within these acute lesions, similar to the value (11,000/ mm^3) reported by Trapp *et al.* (7).

$\text{Na}_v1.6$ and NCX Are Colocalized Within β -APP-Positive Axons in Acute MS Lesions. Electrophysiological studies indicate that reverse operation of the NCX, driven by a persistent sodium influx through sodium channels, can lead to a deleterious accumulation of Ca^{2+} , resulting in degeneration of axons within white matter (10, 11). We have recently demonstrated that $\text{Na}_v1.6$ is colocalized with NCX in β -APP-positive axons in EAE (31). Therefore, we asked whether a similar pattern was present in MS lesions, using triple-label immunocytochemistry to colocalize β -APP with $\text{Na}_v1.6$ and NCX, or with $\text{Na}_v1.2$ and NCX. β -APP-positive axons tended to coexpress $\text{Na}_v1.6$ and NCX (Fig. 5). The percentage of β -APP-positive axons that displayed extensive regions of $\text{Na}_v1.6/\text{NCX}$ immunolabeling (i.e., that displayed both $\text{Na}_v1.6$ and NCX) was $59.4 \pm 5.0\%$ ($n = 4$ patients, 425 axons), significantly greater than the percentage of β -APP-negative axons that displayed $\text{Na}_v1.6/\text{NCX}$ immunolabeling ($18.9 \pm 6.1\%$, $n = 4$ patients, 256 axons; $P < 0.005$) (Figs. 4B and 5). In contrast $\text{Na}_v1.2$ and NCX tended to be coexpressed in β -APP-negative axons; only $18.7 \pm 4.1\%$ of β -APP-positive

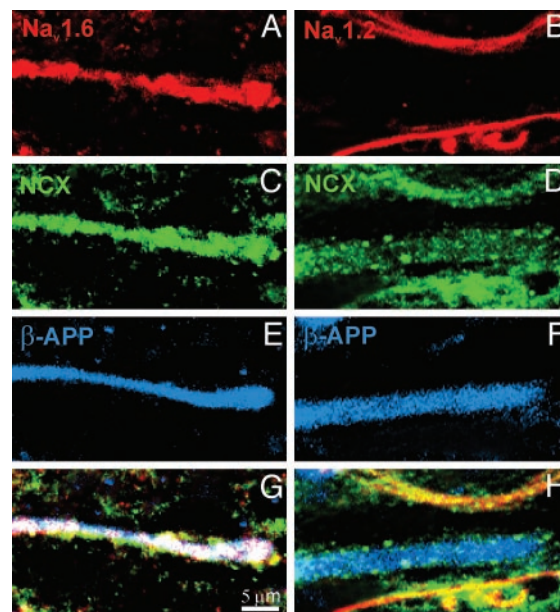


Fig. 5. β -APP-positive spinal cord axons coexpress NCX and $\text{Na}_v1.6$ over extensive regions in acute MS lesions. Digital images demonstrate axons in MS spinal cord white matter immunostained for β -APP (E and F; blue), sodium channel $\text{Na}_v1.6$ (A; red) or $\text{Na}_v1.2$ (B; red), and NCX (C and D; green). G and H correspond to merged images (white). A, C, E, and G show coexpression of $\text{Na}_v1.6$ and NCX within axons displaying β -APP, a marker of axonal injury. In contrast, B, D, F, and H demonstrate NCX-immunopositive staining but an absence of $\text{Na}_v1.2$ immunostaining within β -APP-positive axons, and coexpression of NCX and $\text{Na}_v1.2$ within β -APP-negative axons.

axons coexpressed $\text{Na}_v1.2$ and NCX ($n = 4$ patients, 309 axons), whereas $56.4 \pm 4.8\%$ of β -APP-negative axons coexpressed $\text{Na}_v1.2$ and NCX ($n = 4$ patients, 638 axons; $P < 0.005$) (Figs. 4B and 5). Thus the majority of β -APP-positive axons in MS display extensive regions where both $\text{Na}_v1.6$ and NCX are present, whereas the majority of β -APP-negative axons coexpress $\text{Na}_v1.2$ and NCX.

Discussion

In this study we identify the sodium channels that are expressed along axons within MS lesions. We show that, whereas $\text{Na}_v1.6$ is expressed focally at nodes of Ranvier in control white matter, two sodium-channel isoforms, $\text{Na}_v1.2$ and $\text{Na}_v1.6$, are expressed along extensive regions of demyelinated axons from acute MS lesions. We also demonstrate the selective colocalization of $\text{Na}_v1.6$ and the NCX within axons expressing β -APP, a marker of axonal injury, in MS.

Although lacking in molecular specificity, earlier studies demonstrated that, whereas action-potential generation is confined to the nodal zones where sodium channels are clustered in normal myelinated and acutely demyelinated axons (49–52), some demyelinated axons develop a continuous mode of action-potential conduction, which is supported by a more diffuse distribution of channels (25). Early morphological studies using cytochemical (26) and immunocytochemical labeling methods with pan-specific antibodies, which do not distinguish between subtypes of sodium channels (27–29), demonstrated higher-than-normal densities of sodium channels along extensive regions of demyelinated axons, consistent with the development of continuous conduction. A recent study using subtype-specific antibodies showed that $\text{Na}_v1.2$ and $\text{Na}_v1.6$ are distributed diffusely along extensive regions of demyelinated axons in EAE (4).

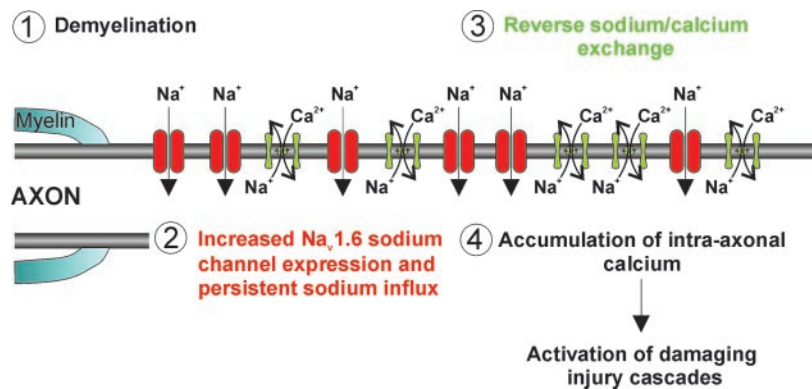


Fig. 6. Proposed mechanism of axonal injury by means of coexpression of $\text{Na}_v1.6$ and NCX. The model suggests that $\text{Na}_v1.6$ sodium channels are up-regulated (1) and expressed along some demyelinated axons, where they produce persistent sodium current (2). The persistent sodium current can drive reverse sodium/calcium exchange (3) and accumulation of intra-axonal calcium (4), triggering injurious secondary cascades and axonal injury.

Based on their physiological properties, it would be expected that $\text{Na}_v1.2$ and $\text{Na}_v1.6$, which both produce rapidly activating and inactivating currents (32–34), would both support action-potential generation. Consistent with this, $\text{Na}_v1.6$ is the predominant sodium channel at nodes of Ranvier (2), whereas $\text{Na}_v1.2$ is expressed along premyelinated CNS axons (3, 22), which are known to conduct action potentials (35, 36). There is evidence suggesting that some sodium channels, when colocalized with the NCX, can contribute to axonal degeneration. Studies in the optic nerve have demonstrated that sustained sodium influx through sodium channels can drive reverse $\text{Na}^+/\text{Ca}^{2+}$ exchange that triggers Ca^{2+} -mediated axonal degeneration (11). Block of sodium channels and of the NCX prevents white matter axon degeneration after a variety of insults (11–15) including injury produced by NO (16, 17), which is present at increased concentrations within MS lesions. In EAE, the sodium-channel blockers phenytoin (18) and flecainide (19) have a protective effect, preventing the degeneration of CNS axons, maintaining axonal conduction, and improving clinical outcome.

Several lines of evidence suggest that $\text{Na}_v1.6$ contributes to the persistent current that drives reverse $\text{Na}^+/\text{Ca}^{2+}$ exchange in injured axons in MS, as suggested in the model illustrated in Fig. 6. Myelinated axons, which are sensitive to injury produced by reverse $\text{Na}^+/\text{Ca}^{2+}$ exchange driven by a persistent Na current (10, 11), express $\text{Na}_v1.6$ at higher levels than other sodium channels (2, 4). In contrast, dysmyelinating CNS axons, which express $\text{Na}_v1.2$ rather than $\text{Na}_v1.6$, (3, 23), are substantially less sensitive than myelinated axons to this type of injury (53). $\text{Na}_v1.6$ channels produce a persistent current in addition to a transient current (33, 37), and the persistent current produced by $\text{Na}_v1.6$ is much larger than the persistent current produced by $\text{Na}_v1.2$ (33). Herzog *et al.* (38) performed patch-clamp analysis on dorsal root ganglion neurons expressing recombinant $\text{Na}_v1.6$ channels and detected persistent $\text{Na}_v1.6$ currents in all cells that were studied. The present results from MS, like recent studies in EAE (31), show an association between expression of $\text{Na}_v1.6$, but not $\text{Na}_v1.2$, and axonal degeneration; $\text{Na}_v1.6$ and the NCX were both, in fact, detectable and colocalized in 60% of β -APP-labeled axons in MS but were found to be coexpressed in <20% of axons that were β -APP-negative. We observed extensive regions of coexpression of $\text{Na}_v1.6$ and NCX often extending for >50 μm ; however, it was not possible to follow single axons for the extent of the entire lesion, and although we predict that the colocalization of $\text{Na}_v1.6$ and NCX induces a focal injury, we cannot exclude a more diffuse process. It might be argued that diffuse $\text{Na}_v1.6$ immunostaining along extensive regions of axons in MS is due

to a damming up of an intracellular pool of $\text{Na}_v1.6$ channels as a result of impaired axoplasmic transport associated with demyelination or axonal injury, rather than insertion of $\text{Na}_v1.6$ channels along the demyelinated axon membrane. However, this argument is not supported by our observations, which indicate that regions of $\text{Na}_v1.6$ expression along demyelinated axons are bounded by Caspr without overlap, as they are in normal myelinated axons (43, 44). Thus we propose that these diffusely expressed $\text{Na}_v1.6$ channels are inserted within the axon membrane and contribute to the model proposed in Fig. 6.

As in our earlier studies in EAE (31), we observed extensive regions of expression of $\text{Na}_v1.6$ in >80% of β -APP-positive axons and coexpression of $\text{Na}_v1.6$ and NCX in a majority of β -APP-positive axons in MS, but were unable to detect these extensive zones of coexpression in the remaining 40% of β -APP-positive axons. Moreover, we observed coexpression of $\text{Na}_v1.6$ and NCX in 18% of β -APP-negative axons. Although we are unable to explain these apparent discrepancies, it should be noted that sodium influx via voltage-gated sodium channels occurs relatively early in the axonal injury cascade (11), possibly earlier than β -APP can be detected, and that, as axonal injury proceeds and axonal protein molecules are degraded, $\text{Na}_v1.6$ and NCX levels may fall below detectable levels (31). Irrespective of this point, the present findings show a high level of coexpression of $\text{Na}_v1.6$ and NCX, but not of $\text{Na}_v1.2$ and NCX, in injured axons in MS.

In the absence of more complete clinical histories, it is not possible to correlate the changes that we have observed in demyelinated axons in MS with clinical status; future studies, in which clinically symptomatic lesions are compared with clinically silent ones, may permit such correlation. We cannot comment, on the basis of the present results, on the mechanisms that determine whether a given axon will express $\text{Na}_v1.6$ or $\text{Na}_v1.2$; neurotrophic factors play a role in regulating neuronal sodium-channel expression (54–56), but other factors may also be involved. Irrespective of this, our results provide a demonstration of molecular plasticity along demyelinated axons in the human CNS in MS, in which the pattern of sodium-channel expression is altered compared with normal myelinated axons. Our results indicate, specifically, that $\text{Na}_v1.2$ and $\text{Na}_v1.6$ are expressed along demyelinated axons in MS and suggest that the presence of these two channel isoforms may affect axonal function in different ways.

M.J.C. thanks Medical Director General, U.K., for support. We thank Dr. Matthew Rasband for the generous gift of Caspr antibody and critical appraisal of the manuscript, and Lynda Tyrell, Pamela Zwinger, and Bart

Toftness for excellent technical assistance. This work was supported in part by grants from the National Multiple Sclerosis Society and the Medical Research Service and Rehabilitation Research Service, De-

partment of Veteran Affairs, and by gifts from the Paralyzed Veterans of America, the United Spinal Association, and the Nancy Davis Foundation.

1. Goldin, A. L., Barchi, R. L., Caldwell, J. H., Hofmann, F., Howe, J. R., Hunter, J. C., Kallen, R. G., Mandel, G., Meisler, M. H., Netter, Y. B., et al. (2000) *Neuron* **28**, 365–368.
2. Caldwell, J. H., Schaller, K. L., Lasher, R. S., Peles, E. & Levinson, S. R. (2000) *Proc. Natl. Acad. Sci. USA* **97**, 5616–5620.
3. Boiko, T., Rasband, M. N., Levinson, S. R., Caldwell, J. H., Mandel, G., Trimmer, J. S. & Matthews, G. (2001) *Neuron* **30**, 91–104.
4. Craner, M. J., Lo, A. C., Black, J. A. & Waxman, S. G. (2003) *Brain* **126**, 1552–1561.
5. Waxman, S. G. (1998) *N. Engl. J. Med.* **338**, 323–325.
6. Ferguson, B., Matyszak, M. K., Esiri, M. M. & Perry, V. H. (1997) *Brain* **120**, 393–399.
7. Trapp, B. D., Peterson, J., Ransohoff, R. M., Rudick, R., Mork, S. & Bo, L. (1998) *N. Engl. J. Med.* **338**, 278–285.
8. Lovas, G., Szilagyi, N., Majtenyi, K., Palkovits, M. & Komoly, S. (2000) *Brain* **123**, 308–317.
9. Bjartmar, C., Kidd, G., Mork, S., Rudick, R. & Trapp, B. D. (2000) *Ann. Neurol.* **48**, 893–901.
10. Stys, P. K., Sontheimer, H., Ransom, B. R. & Waxman, S. G. (1993) *Proc. Natl. Acad. Sci. USA* **90**, 6976–6980.
11. Stys, P. K., Waxman, S. G. & Ransom, B. R. (1992) *J. Neurosci.* **12**, 430–439.
12. Stys, P. K., Ransom, B. R. & Waxman, S. G. (1992) *J. Neurophysiol.* **67**, 236–240.
13. Imaizumi, T., Kocsis, J. D. & Waxman, S. G. (1998) *Brain Res.* **779**, 292–296.
14. Agrawal, S. K. & Fehlings, M. G. (1996) *J. Neurosci.* **16**, 545–552.
15. Rosenberg, L. J., Teng, Y. D. & Wrathall, J. R. (1999) *J. Neurosci.* **19**, 6122–6133.
16. Garthwaite, G., Goodwin, D. A., Batchelor, A. M., Leeming, K. & Garthwaite, J. (2002) *Neuroscience* **109**, 145–155.
17. Kapoor, R., Davies, M., Blaker, P. A., Hall, S. M. & Smith, K. J. (2003) *Ann. Neurol.* **53**, 174–180.
18. Lo, A. C., Saab, C. Y., Black, J. A. & Waxman, S. G. (2003) *J. Neurophysiol.* **90**, 3566–3571.
19. Bechtold, D. A., Kapoor, R. & Smith, K. J. (2004) *Ann. Neurol.* **55**, 607–616.
20. Westenbroek, R. E., Merrick, D. K. & Catterall, W. A. (1989) *Neuron* **3**, 695–704.
21. Gong, B., Rhodes, K. J., Bekele-Arcuri, Z. & Trimmer, J. S. (1999) *J. Comp. Neurol.* **412**, 342–352.
22. Kaplan, M. R., Cho, M. H., Ullian, E. M., Isom, L. L., Levinson, S. R. & Barres, B. A. (2001) *Neuron* **30**, 105–119.
23. Westenbroek, R. E., Noebels, J. L. & Catterall, W. A. (1992) *J. Neurosci.* **12**, 2259–2267.
24. Rasband, M. N., Kagawa, T., Park, E. W., Ikenaka, K. & Trimmer, J. S. (2003) *J. Neurosci. Res.* **73**, 465–470.
25. Bostock, H. & Sears, T. A. (1978) *J. Physiol.* **280**, 273–301.
26. Foster, R. E., Whalen, C. C. & Waxman, S. G. (1980) *Science* **210**, 661–663.
27. Novakovic, S. D., Levinson, S. R., Schachner, M. & Shrager, P. (1998) *Muscle Nerve* **21**, 1019–1032.
28. England, J. D., Gamboni, F. & Levinson, S. R. (1991) *Brain Res.* **548**, 334–337.
29. England, J. D., Gamboni, F., Levinson, S. R. & Finger, T. E. (1990) *Proc. Natl. Acad. Sci. USA* **87**, 6777–6780.
30. Moll, C., Murre, C., Lazdunski, M. & Ulrich, J. (1991) *Brain Res.* **556**, 311–316.
31. Craner, M. J., Hains, B. C., Lo, A. C., Black, J. A. & Waxman, S. G. (2004) *Brain* **127**, 294–303.
32. Auld, V. J., Goldin, A. L., Krafte, D. S., Marshall, J., Dunn, J. M., Catterall, W. A., Lester, H. A., Davidson, N. & Dunn, R. J. (1988) *Neuron* **1**, 449–461.
33. Smith, M. R., Smith, R. D., Plummer, N. W., Meisler, M. H. & Goldin, A. L. (1998) *J. Neurosci.* **18**, 6093–6102.
34. Stuhmer, W., Conti, F., Suzuki, H., Wang, X. D., Noda, M., Yahagi, N., Kubo, H. & Numa, S. (1989) *Nature* **339**, 597–603.
35. Foster, R. E., Connors, B. W. & Waxman, S. G. (1982) *Brain Res.* **255**, 371–386.
36. Rasband, M. N., Peles, E., Trimmer, J. S., Levinson, S. R., Lux, S. E. & Shrager, P. (1999) *J. Neurosci.* **19**, 7516–7528.
37. Burbidge, S. A., Dale, T. J., Powell, A. J., Whitaker, W. R., Xie, X. M., Romanos, M. A. & Clare, J. J. (2002) *Mol. Brain Res.* **103**, 80–90.
38. Herzog, R. I., Cummins, T. R., Ghassemi, F., Dib-Hajj, S. D. & Waxman, S. G. (2003) *J. Physiol.* **551**, 741–750.
39. Newcombe, J. & Cuzner, M. L. (1993) *J. Neural Transm. Suppl.* **39**, 155–163.
40. Li, H., Newcombe, J., Groome, N. P. & Cuzner, M. L. (1993) *Neuropathol. Appl. Neurobiol.* **19**, 214–223.
41. Steffensen, I., Waxman, S. G., Mills, L. & Stys, P. K. (1997) *Brain Res.* **776**, 1–9.
42. Bagasra, O., Michaels, F. H., Zheng, Y. M., Bobroski, L. E., Spitsin, S. V., Fu, Z. F., Tawadros, R. & Koprowski, H. (1995) *Proc. Natl. Acad. Sci. USA* **92**, 12041–12045.
43. Einheber, S., Zanazzi, G., Ching, W., Scherer, S., Milner, T. A., Peles, E. & Salzer, J. L. (1997) *J. Cell Biol.* **139**, 1495–1506.
44. Bhat, M. A., Rios, J. C., Lu, Y., Garcia-Fresco, G. P., Ching, W., St. Martin, M., Li, J., Einheber, S., Chesler, M., Rosenbluth, J., et al. (2001) *Neuron* **30**, 369–383.
45. Arroyo, E. J., Xu, T., Grinspan, J., Lambert, S., Levinson, S. R., Brophy, P. J., Peles, E. & Scherer, S. S. (2002) *J. Neurosci.* **22**, 1726–1737.
46. Black, J. A., Renganathan, M. & Waxman, S. G. (2002) *Brain Res. Mol. Brain Res.* **105**, 19–28.
47. Bitsch, A., Schuchardt, J., Bunkowski, S., Kuhlmann, T. & Bruck, W. (2000) *Brain* **123**, 1174–1183.
48. Kuhlmann, T., Lingfeld, G., Bitsch, A., Schuchardt, J. & Bruck, W. (2002) *Brain* **125**, 2202–2212.
49. Rasminsky, M. & Sears, T. A. (1972) *J. Physiol.* **227**, 323–350.
50. Ritchie, J. M. & Rogart, R. B. (1977) *Proc. Natl. Acad. Sci. USA* **74**, 211–215.
51. Waxman, S. G. (1977) *Arch. Neurol. (Chicago)* **34**, 585–589.
52. Shrager, P. (1989) *Brain Res.* **483**, 149–154.
53. Waxman, S. G., Davis, P. K., Black, J. A. & Ransom, B. R. (1990) *Ann. Neurol.* **28**, 335–340.
54. Dib-Hajj, S. D., Black, J. A., Cummins, T. R., Kenney, A. M., Kocsis, J. D. & Waxman, S. G. (1998) *J. Neurophysiol.* **79**, 2668–2676.
55. Toledo-Aral, J. J., Brehm, P., Halegoua, S. & Mandel, G. (1995) *Neuron* **14**, 607–611.
56. Boucher, T. J., Okuse, K., Bennett, D. L., Munson, J. B., Wood, J. N. & McMahon, S. B. (2000) *Science* **290**, 124–127.